

Identifying Vector Field Singularities Using a Discrete Hodge Decomposition

Konrad Polthier and Eike Preuß

Technical University Berlin, Institute of Mathematics, MA 8-3, 10623 Berlin **

Summary. We derive a Hodge decomposition of discrete vector fields on polyhedral surfaces, and apply it to the identification of vector field singularities. This novel approach allows us to easily detect and analyze singularities as critical points of corresponding potentials. Our method uses a global variational approach to independently compute two potentials whose gradient respectively co-gradient are rotation-free respectively divergence-free components of the vector field. The sinks and sources respectively vortices are then automatically identified as the critical points of the corresponding scalar-valued potentials. The global nature of the decomposition avoids the approximation problem of the Jacobian and higher order tensors used in local methods, while the two potentials plus a harmonic flow component are an exact decomposition of the vector field containing all information.

1 Introduction and Related Work

Singularities of vector fields are among the most important features of flows. They determine the physical behavior of flows and allow one to characterize the flow topology [9][10]. The most prominent singularities are sinks, sources, and vortices. Higher order singularities often appear in magnetic fields. All these singularities must be detected and analyzed in order to understand the physical behavior of a flow or in order to use them as an ingredient for many topology-based algorithms [24][26]. Although feature analysis is an important area, only a few technical tools are available for the detection of singularities and their visualization.

Methods for direct vortex detection are often based on the assumption that there are regions with high amounts of rotation or divergence. See, for example, Banks and Singer [1] for an overview of possible quantities to investigate. The deficiencies of first-order approximations have been widely recognized, and, for example, higher-order methods try to overcome this problem [18]. The detection and visualization of higher-order singularities is an active research area where rather heavy mathematical methods have been employed [21].

The Jacobian $\nabla\xi$ of a differentiable vector field ξ in \mathbb{R}^2 or \mathbb{R}^3 can be decomposed into a stretching tensor S and a vorticity matrix Ω , the symmetric and anti-symmetric parts of $\nabla\xi$. The eigenvalues of the diagonal matrix S correspond to the compressibility of the flow, and the off-diagonal entries

** polthier@math.tu-berlin.de, eike@sfb288.math.tu-berlin.de

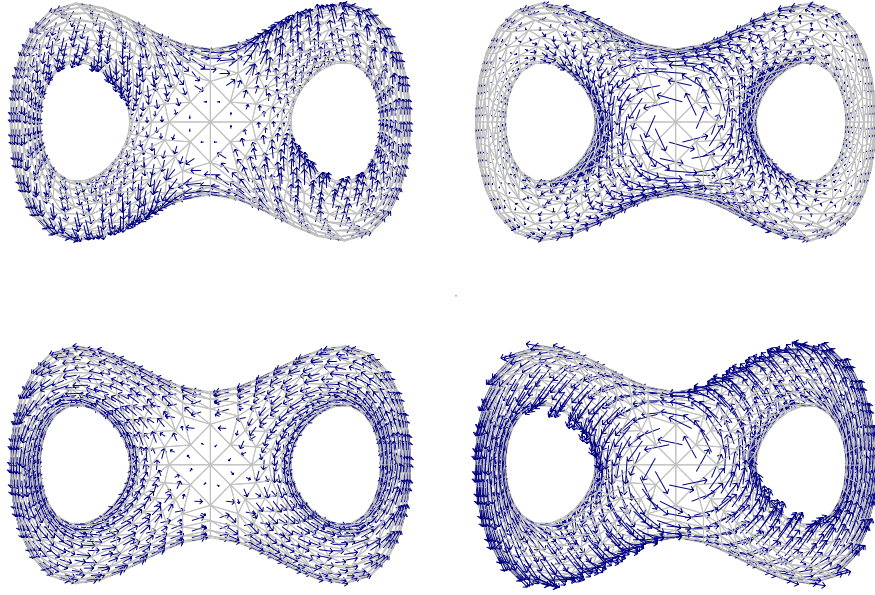


Fig. 1. Pretzel in \mathbb{R}^3 with vector field, obtained by projection of a flow around the z-axis onto the tangential space of the curved, 2-dimensional surface. Original field (bottom right), rotation-free component (upper left) and divergence-free component (upper right). The harmonic component (bottom left) belongs to an incompressible, rotation-free flow around the handles of the pretzel. See also Sect. 7.

of Ω are the components of the rotation vector. This matrix decomposition has classically also been used for discrete vector fields where the Jacobian is approximated by discrete difference techniques. The quality of this approach depends on the quality of the underlying grid and the accuracy of the vector field. For practical problems of vortex identification we refer to the case study of Kenwright and Haines [12], and the eigenvector method in Sujudi and Haines [22].

Another class of methods follows a geometric approach where geometric properties of streamlines and pathlines are investigated and put in relation to properties of the flow [19][20]. Tittgemeyer et al. [23] use a contraction mapping to detect singularities of displacement fields in magnetic resonance imaging. This helps in the understanding of pathological processes in a brain. Their method is applicable to any higher order singularities but fails to detect some critical points like centers of rotation or balanced saddle points.

Our approach uses a discrete version of the Hodge-Helmholtz decomposition of vector fields on curved surfaces M_h . We choose a global variational

approach to compute the decomposition of a discrete vector field ξ which seems to be a novel approach to the detection and analysis of singularities of discrete vector fields. We compute two potentials u and w which determine the rotation-free and the divergence-free components of the flow. The remaining harmonic component v comprises the incompressible and irrotational component of the flow such that we have the exact decomposition (see Theorem 5)

$$\xi = \nabla u + \delta(w\omega) + v.$$

The potentials are obtained by a global variational approach where certain energy functionals are minimized in the set of scalar-valued functions on the surface M_h . The detection and analysis of vector field singularities is then transferred to the much simpler study of the critical points of the scalar valued potentials. In contrast to local methods, our approach avoids the approximation of the Jacobian matrix or higher order tensors from local information.

Although the Helmholtz decomposition [11] of smooth fields into a curl-free and divergence-free part is well-known in fluid dynamics [5], we have not found any application to the study of singularities of discrete vector fields. Discrete differential forms were introduced in differential geometry by Whitney [25] who invented the so-called Whitney forms. Whitney forms were brought to a new life in the pioneering work on discrete Hodge decompositions in computational electromagnetism by Bossavit [3][2] who applied them to the solution of boundary value problems. For simplicial complexes, Eckmann [8] developed a combinatorial Hodge theory. Dodziuk [7] showed that if a simplicial complex K is a smooth triangulation of a compact oriented Riemann manifold X then the combinatorial Hodge theory is an approximation of the Hodge theory of forms on X by choosing a suitable inner product on K .

Our discretization method has connections with weak derivatives used in finite element theory where the formal application of partial integration is used to shift the differentiation operation to differentiable test functions. In fact, the integrands of our discrete differential operators div_h and rot_h can be obtained from $\nabla\xi$ by formal partial integration with test functions. In contrast, our focus here is to emphasize the geometric interpretation of the discrete differentials, and to relate them with the discrete Hodge operator which also played a role in the discrete minimal surface theory in Polthier [15].

In Sect. 7 we apply our method to several test cases with artificial and simulated flows which are accurately analyzed. The simulated flow in the Bay of Gdansk reproduces similar results of Post and Sadarjoen [19], who applied different geometric methods.

2 Setup

In the following let M_h be a simplicial surface immersed in \mathbb{R}^n (possibly with self-intersections and/or boundary), that is a surface consisting of planar triangles where the topological neighbourhood of any vertex consists of a collection of triangles homeomorphic to a disk (see [15] for an exact definition of a simplicial surface). We need the following finite element spaces, see the books [6][4] for an introduction.

Definition 1. *On a simplicial surface M_h we define the function space S_h of conforming finite elements:*

$$S_h := \{v : M_h \rightarrow \mathbb{R} \mid v \in C^0(M_h) \text{ and } v \text{ is linear on each triangle}\}$$

S_h is a finite dimensional space spanned by the Lagrange basis functions $\{\varphi_1, \dots, \varphi_n\}$ corresponding to the set of vertices $\{p_1, \dots, p_n\}$ of M_h , that is for each vertex p_i we have a function

$$\begin{aligned} \varphi_i : M_h &\rightarrow \mathbb{R}, \varphi_i \in S_h \\ \varphi_i(p_j) &= \delta_{ij} \quad \forall i, j \in \{1, \dots, n\} \\ \varphi_i &\text{ is linear on each triangle.} \end{aligned} \tag{1}$$

Then each function $u_h \in S_h$ has a unique representation

$$u_h(p) = \sum_{j=1}^n u_j \varphi_j(p) \quad \forall p \in M_h$$

where $u_j = u_h(p_j) \in \mathbb{R}$. The function u_h is uniquely determined by its nodal vector $(u_1, \dots, u_n) \in \mathbb{R}^n$.

The space of non-conforming finite elements includes discontinuous functions such that their use is still sometimes titled as a *variational crime* in the finite element literature. Nevertheless, non-conforming functions naturally appear in the Hodge decomposition and in the theory of discrete minimal surfaces [15].

Definition 2. *For a simplicial surface M_h , we define the space of non-conforming finite elements by*

$$S_h^* := \left\{ v : M_h \rightarrow \mathbb{R} \mid \begin{array}{l} v|_T \text{ is linear for each } T \in M_h, \text{ and} \\ v \text{ is continuous at all edge midpoints} \end{array} \right\}$$

The space S_h^* is no longer a finite dimensional subspace of $H^1(M_h)$ as in the case of conforming elements, but S_h^* is a superset of S_h . Let $\{m_i\}$ denote the set of edge midpoints of M_h , then for each edge midpoint m_i we have a basis function

$$\begin{aligned} \psi_i : M_h &\rightarrow \mathbb{R} \quad \psi_i \in S_h^* \\ \psi_i(m_j) &= \delta_{ij} \quad \forall i, j \in \{1, 2, \dots\} \\ \psi_i &\text{ is linear on each triangle.} \end{aligned} \tag{2}$$

The support of a function ψ_i consists of the (at most two) triangles adjacent to the edge e_i , and ψ_i is usually not continuous on M_h . Each function $v \in S_h^*$ has a representation

$$v_h(p) = \sum_{\text{edges } e_i} v_i \psi_i(p) \quad \forall p \in M_h$$

where $v_i = v_h(m_i)$ is the value of v_h at the edge midpoint m_i of e_i .

We use the following space of vector fields on M_h

$$A_h^1 := \{v \mid v|_T \text{ is a constant, tangential vector on each triangle}\}$$

which will later be considered in the wider setup of discrete differential forms. As common practice in the finite element context, the subindex h distinguishes this set from smooth concepts.

On each oriented triangle, we define the operator J that rotates each vector by an angle $\frac{\pi}{2}$ on the oriented surface.

Note, in this paper we use a slightly more general definition of the spaces S_h respectively S_h^* , namely we include functions which are only defined at vertices respectively at edge midpoints. For example, the (total) Gauß curvature is defined solely at vertices. Here for a given vector field ξ we will have $\text{div}_h \xi \in S_h$ (respectively $\text{div}_h^* \xi \in S_h^*$) to be defined solely at a vertex. The motivation of this generalization is two-fold: first, a simplified notation of many statements, and, second, the fact that for visualization purposes one often extends these point-based values over the surface. For example, barycentric interpolation allows to color the interior of triangles based on the discrete Gauss curvature at its vertices. Caution should be taken if integral entities are derived.

3 Discrete Rotation

The rotation rot of a differentiable vector field on a smooth surfaces is at each point p a vector normal to the surface whose length measures the angular momentum of the flow. On a planar Euclidean domain with local coordinates (x, y) , the rotation of a differentiable vector field $v = (v_1, v_2)$ is given by $\text{rot } v = (0, 0, \frac{\partial}{\partial x} v_2 - \frac{\partial}{\partial y} v_1)$. In the discrete version of this differential operators, the (total) discrete rotation, we neglect the vectorial aspect and consider the rotation as a scalar value given by the normal component.

In the following we use a simplicial domain M_h which contains its boundary. The boundary is assumed to be counter clockwise parametrized. If $p \in \partial M_h$ is a vertex on the boundary then $\text{star } p$ consists of all triangles containing p . If $m \in \partial M_h$ is the midpoint of an edge c then $\partial \text{star } m$ does contain the edge c as well.

Definition 3. Let $v \in \Lambda_h^1$ be a piecewise constant vector field on a simplicial surface M_h . Then the (total) discrete rotation $\text{rot } v$ is a vertex based function in S_h given by

$$\text{rot}_h v(p) := \frac{1}{2} \int_{\partial \text{star } p} v = \frac{1}{2} \sum_{i=1}^k \langle v, c_i \rangle$$

where c_i are the edges of the oriented boundary of the star of $p \in M_h$.

Additionally, the discrete rotation $\text{rot}^* v$ at the midpoint m of each edge c is an edge-midpoint based function in S_h^* given by

$$\text{rot}_h^* v(m) := \int_{\partial \text{star } c(m)} v$$

where $\partial \text{star } m$ is the oriented boundary of the triangles adjacent to edge c .

If the rotation of a vector field is positive on each edge of the link of a vertex then the vector field rotates counter clockwise around this vertex. Note that $\text{rot}_h^* v$ vanishes along the boundary. One easily shows the following Lemma.

Lemma 1. Let p be a vertex of a simplicial surface M_h with emanating edges $\{c_1, \dots, c_k\}$ with edge midpoints m_i . Then

$$2\text{rot}_h v(p) = \sum_{i=1}^k \text{rot}_h^* v(m_i) .$$

Note, that $\text{rot}_h^* v = 0$ at all edge midpoints implies $\text{rot}_h v = 0$ on all vertices. The converse is not true in general.

Rotation-free vector fields are characterized by the existence of a discrete potential.

Theorem 1. Let M_h be a simply connected simplicial surface with a piecewise constant vector field v . Then $v = \nabla u$ is the gradient of a function $u \in S_h$ if and only if

$$\text{rot}_h^* v(m) = 0 \quad \forall \text{ edge midpoints } m .$$

Similarly, $v = \nabla u^*$ is the gradient of a function $u^* \in S_h^*$ if and only if

$$\text{rot}_h v(p) = 0 \quad \forall \text{ interior vertices } p .$$

Further, for a vertex $q \in \partial M_h$ the value $\text{rot}_h \nabla u^*(q)$ is the difference of $u^*(q)$ at the two adjacent boundary triangles.

Proof. 1.) ” \Rightarrow ”: Assume the orientation of the common edge $c = T_1 \cap T_2$ of two triangles leads to a positive orientation of ∂T_1 . Then we obtain from the definition of $\text{rot}_h^* v$

$$\text{rot}_h^* v(m) = - \langle v|_{T_1}, c \rangle + \langle v|_{T_2}, c \rangle .$$

Let T_1 be a triangle with vertices $\{p_1, p_2, p_3\}$ and edges $c_j = p_{j-1} - p_{j+1}$. Assume $v = \nabla u_h$ is the gradient of a piecewise linear function $u_h \in S_h$. Let $u_j = u_h(p_j)$ be the function values at the vertices of T_1 then

$$\langle \nabla u_h, c_j \rangle = u_{j-1} - u_{j+1} .$$

The sum of the two scalar products $\langle \nabla u_h, c \rangle$ at the common edge of two adjacent triangles cancels because of the continuity of u_h and the reversed orientation of c in the second triangle.

" \Leftarrow ": We construct a vertex spanning tree of M_h and orient its edges towards the root of the tree. Since v is rotation-free the scalar product of v with each oriented edge c_j is unique, and we denote it with $v_j := \langle v, c_j \rangle$. Now we construct a function u_h by assigning $u_h(r) := 0$ at the root of the spanning tree, and integrate along the edges of the spanning tree such that

$$u_h(p_{j_2}) - u_h(p_{j_1}) = v_j$$

if $c_j = p_{j_2} - p_{j_1}$. This leads to a function $u_h \in S_h$. On each triangle T we have $\nabla u|_T = v|_T$ since by construction we have $\langle \nabla u_h, c_j \rangle = u_h(p_{j_2}) - u_h(p_{j_1}) = v_j$ on each edge c_j .

We now show that the function u_h is independent of the choice of the spanning tree. It is sufficient to show that the integration is path independent on each triangle (which is clear) and around the link of each vertex. Around a vertex p denote the vertices of its oriented link with $\{q_1, \dots, q_s\}$. Since we have the edge differences $u(p) - u(q_j) = v_j$ it follows that

$$\begin{aligned} \sum_{j=1}^s u(q_j) - u(q_{j+1}) &= \sum_{j=1}^s u(q_j) - u(p) + u(p) - u(q_{j+1}) \\ &= \sum_{j=1}^s -v_j + v_{j+1} = 0 . \end{aligned}$$

The function u_h depends solely on v and the integration constant $u_h(r)$.

2.) The second assumption follows from a similar calculation which we only sketch here.

" \Rightarrow ": If v is the gradient of a function $u^* \in S_h^*$ then the assumption follows since at all interior vertices p we have

$$\begin{aligned} \int_{\gamma_p} \nabla u^* &= \sum_{j=1}^n \langle \nabla u^*, m_j - m_{j-1} \rangle \\ &= \sum_{j=1}^n u^*(m_j) - u^*(m_{j-1}) = 0 \end{aligned}$$

where γ_p is a polygon connecting the midpoints m_j of all edges emanating from p .

” \Leftarrow ” By assumption, the path integral of v along any closed curve γ crossing edges at their midpoints vanishes. Since v integrates to a linear function on each triangle, we obtain a well-defined function $u_h^* \in S_h^*$ similar to the procedure in 1.) by

$$u_h^*(p) := \int_{\gamma} v$$

where γ is any path from a base point $r \in M_h$ to p which crosses edges at their midpoints.

3.) The statement on the height difference of u^* at a boundary vertex q follows directly from the evaluation of $\text{rot}_h \nabla u^*(q)$.

The above theorem does not hold for non-simply connected surfaces since integration along closed curves, which are not null-homotopic, may lead to periods. Also note, that from $S_h \subset S_h^*$ follows $0 = \text{rot}_h \nabla u = \text{rot}_h^* \nabla u$ for any $u \in S_h$.

4 Discrete Divergence

In the smooth case the divergence div of a field is a real-valued function measuring at each point p on a surface the amount of flow generated in an infinitesimal region around p . On a planar Euclidean domain with local coordinates (x, y) , the divergence of a differentiable vector field $v = (v_1, v_2)$ is given by $\text{div } v = v_{1|x} + v_{2|y}$. The discrete version of this differential operators, the (total) discrete divergence, is obtained by a similar physical reasoning, that means we define the discrete divergence as the amount of flow generated inside the star p of a vertex p which is the total amount flowing through the boundary of star p .

At a boundary vertex p the discrete divergence must take into account the flow through the two boundary edges as well as divergence generated at all other edges emanating from p since the divergence at these interior edges has only been considered by half at interior vertices. The following definition also fulfills the formal integration by parts relation (3):

Definition 4. *Let $v \in \Lambda_h^1$ be a piecewise constant vector field on a simplicial surface M_h . Then the (total) discrete divergence $\text{div}_h : \Lambda_h^1 \rightarrow S_h$ of v is a vertex-based function given by*

$$\text{div}_h v(p) = \frac{1}{2} \int_{\partial \text{star } p} \langle v, \nu \rangle ds$$

where ν is the exterior normal along the oriented boundary of the star of $p \in M_h$. If $p \in \partial M_h$ then $\text{star } p$ consists of all triangles containing p .

Additionally, we define the divergence operator $\text{div}_h^* : \Lambda_h^1 \rightarrow S_h^*$ based at the midpoint m of an edge c

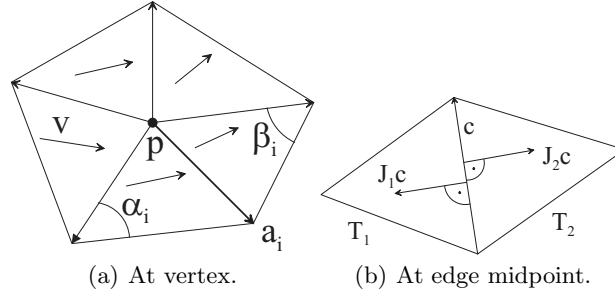


Fig. 2. On the definition of discrete divergence.

$$\operatorname{div}_h^* v(m) = \int_{\partial \operatorname{star} m} \langle v, \nu \rangle ds$$

where $\partial \operatorname{star} m$ is the oriented boundary of the triangles adjacent to edge c . If $m \in \partial M_h$ then $\partial \operatorname{star} m$ does not contain the edge c .

Note, the divergence div_h^* at an edge c common to two triangles T_1 and T_2 may equivalently be defined by $\operatorname{div}_h^* v(m) = \langle v, Jc_1 \rangle_{|T_1} + \langle v, Jc_2 \rangle_{|T_2}$ where the common edge has opposite orientation $c_1 = -c_2$ in each triangle. Let $\varphi_p \in S_h$ denote the Lagrange basis function associated to each vertex p of M_h . Then formally, the discrete divergence can be obtained by applying Green's integration by parts

$$\begin{aligned} \operatorname{div}_h v(p) &:= \int_{\operatorname{star} p} \text{"div } v\text{"} \cdot \varphi_p dx \\ &= - \int_{\operatorname{star} p} \langle v, \nabla \varphi_p \rangle dx + \int_{\partial \operatorname{star} p} \langle v, \nu \rangle \varphi_p ds \end{aligned} \quad (3)$$

although Green's formula does not hold in the discrete setting since v and φ_p are not differentiable on $\operatorname{star} p$. On the right hand side the boundary integral vanishes since $\varphi_p = 0$ along $\partial \operatorname{star} p$ such that we obtain the same equation for $\operatorname{div}_h v(p)$ as in definition above.

The normalization of the divergence operator gives the following equality known from the smooth case:

$$\operatorname{div}_h \nabla u_h = \Delta_h u_h \quad (4)$$

using the discrete Laplace operator Δ_h in [13]. The same holds for the operators on S_h^* .

The discrete version of the Gauß integration theorem relates the divergence of a domain to the flow through its boundary.

Theorem 2. *Let M_h be a simplicial surface with boundary ∂M_h and piecewise constant vector field v . Then*

$$\sum_{p \in M_h} \operatorname{div}_h v(p) = \int_{\partial M_h} \langle v, \nu \rangle \quad (5)$$

where ν is the exterior normal along ∂M_h . Further, we have

$$\sum_{m \in M_h} \operatorname{div}_h^* v(m) = \int_{\partial M_h} \langle v, \nu \rangle \quad (6)$$

where m runs through the midpoints of all edges of M_h .

Proof. Sort and count edges, using that the integral along all edges of a single triangle vanishes.

For practical applications, we compute the explicit formula for the discrete divergence operator in terms of triangle quantities. Note the similarity with the formula of the discrete Laplace operator [13] where the influence of the domain metric solely appears in the cotangent factor.

Theorem 3. *Let $v \in \Lambda_h^1$ be a piecewise constant vector field on a simplicial surface M_h . Then the discrete divergence div_h of v is given at each vertex p by*

$$\operatorname{div}_h v(p) = -\frac{1}{2} \sum_{i=1}^k \langle v, Jc_i \rangle = \frac{1}{2} \sum_{i=1}^k (\cot \alpha_i + \cot \beta_i) \langle v, a_i \rangle \quad (7)$$

where J denotes the rotation of a vector by $\frac{\pi}{2}$ in each triangle, k the number of directed edges a_i emanating from p , and the edges c_i form the closed cycle of $\partial \operatorname{star} p$ in counter clockwise order. In the two triangles adjacent to an edge a_i we denote the vertex angles at the vertices opposite to a_i with α_i and β_i (see Fig. 2).

Proof. By definition Jc rotates an edge such that it points into the triangle, i.e. $Jc = -\nu|c|$ is in opposite direction of the outer normal of the triangle at c . Therefore, the representation of the discrete divergence operator follows from the representation of

$$Jc = \cot \alpha a + \cot \beta b$$

in each triangle with edges $c = a - b$, and sorting the terms around star p by edges.

Lemma 2. *The discrete rotation and divergence of a vector field $v \in \Lambda_h^1$ on a simplicial surface M_h relate by*

$$\operatorname{rot}_h Jv(p) = \operatorname{div}_h v(p),$$

respectively,

$$\operatorname{rot}_h^* Jv(m) = \operatorname{div}_h^* v(m)$$

where p is a vertex and m is the midpoint an edge of M_h .

Proof. The two relations of rot and div follow directly from definitions 4 and 3 of the differential operators.

The divergence at vertices and edges is related by the following lemma.

Lemma 3. *Let p be a vertex of simplicial surface M_h with emanating edges $\{c_1, \dots, c_k\}$ with edge midpoints m_i . Then*

$$2\operatorname{div}_h v(p) = \sum_{i=1}^k \operatorname{div}_h^* v(m_i).$$

Proof. On a single triangle we have $\operatorname{div}_h^* v(m_3) = -\operatorname{div}_h^* v(m_1) - \operatorname{div}_h^* v(m_2)$. Therefore, the right-hand side of the assumed equation is equal to

$$\int_{\partial \operatorname{star} p} \langle v, \nu \rangle$$

as assumed.

Divergence-free vector fields in \mathbb{R}^2 can be characterized by the existence of a discrete 2-form ω with $\delta(\omega) = v$ (where δ is the co-differential operator, see also Def. 7) which is another justification of the discrete definition of div_h . Here we formulate the statement without the usage of differential forms which are introduced in the next section.

Theorem 4. *Let v be a piecewise constant vector field on a simply connected simplicial surface M_h . Then*

$$\operatorname{div}_h v(p) = 0 \quad \forall \text{ interior vertices } p$$

if and only if there exists a function $u^ \in S_h^*$ with $v = J\nabla u^*$. Respectively,*

$$\operatorname{div}_h^* v(m) = 0 \quad \forall \text{ edge midpoints } m$$

if and only if there exists a function $u \in S_h$ with $v = J\nabla u$. In both cases, the function is unique up to an integration constant.

Proof. Using the relation between the discrete rotation and divergence of Lemma 2 the statement follows directly from the integrability conditions proven in Theorem 1.

5 Hodge Type Decomposition of Vector Fields

On each triangle we have a well-defined volume form ω from the induced metric of the triangle which can be expressed as $\omega = \nabla x \wedge \nabla y$ in local orthonormal coordinates (x, y) of the triangle, and for each vector v a one-form v which can be expressed as $v_1 \nabla x + v_2 \nabla y$.

Definition 5. The spaces of discrete differential forms on a simplicial surface M_h are defined piecewise per triangle T :

$$\begin{aligned} \Lambda_h^0 &:= \{u : M_h \rightarrow \mathbb{R} \mid u \text{ is continuous and } u|_T \text{ linear}\} \cong S_h \\ \Lambda_h^1 &:= \{v \mid v|_T \text{ is a constant, tangential vector}\} \\ \Lambda_h^2 &:= \left\{ w \mid \begin{array}{l} \text{on each simply connected region } D \\ w|_D = u\omega \text{ with a function } u \in \Lambda^0 \end{array} \right\}. \end{aligned}$$

Additionally, we define the spaces $\Lambda^{0,*} \supset \Lambda^0$ and $\Lambda^{2,*} \supset \Lambda^2$ having functional representatives in S_h^* .

The space Λ_h^1 is the space of discrete vector fields on a polyhedral surface which are tangential and constant on each triangle. In the following we try to avoid too much formalism and, on simply connected domains, identify a 2-form $w = u\omega$ with its function u without explicitly listing the volume form ω . Similarly, we identify vector fields with 1-forms.

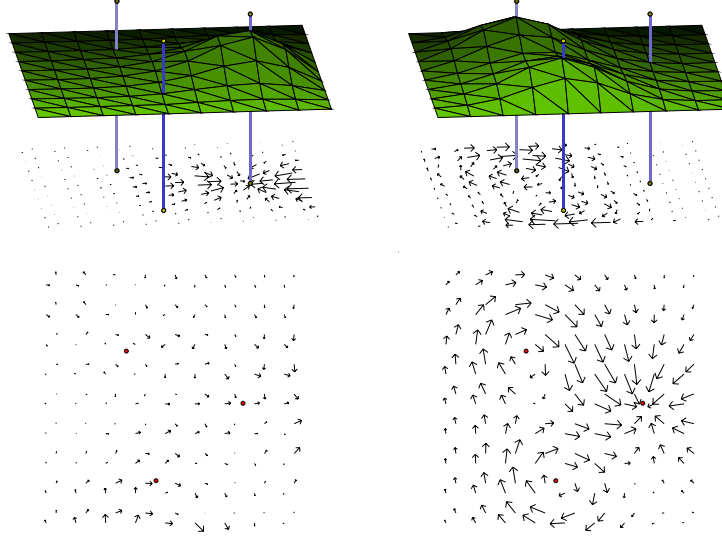


Fig. 3. Test vector field (bottom right) decomposed in rotation-free (upper left), divergence-free (upper right) and harmonic component (bottom left). The three lines indicate the centers of the original potentials.

Definition 6. On a simplicial surface M_h the Hodge operator $*$ is a map

$$* : \Lambda_h^i \rightarrow \Lambda_h^{2-i}$$

such that locally

$$\begin{aligned} *u &= u\omega \quad \forall u \in \Lambda_h^0 \text{ respectively } \Lambda_h^{0,*} \\ *v &= Jv \quad \forall v \in \Lambda_h^1 \\ *(u\omega) &= u \quad \forall (u\omega) \in \Lambda_h^2 \text{ respectively } \Lambda_h^{2,*} . \end{aligned}$$

The gradient operator ∇ used in S_h^* generalizes to two differential operators ∇ and δ on differential forms. We use rot_h^* respectively div_h in order to synchronize with the integrability condition of discrete vector fields in the following sequences.

Definition 7. The differential operator $\nabla : \Lambda_h^0 \rightarrow \Lambda_h^1 = \Lambda_h^{1,*} \rightarrow \Lambda_h^{2,*}$ on a simplicial surface M_h is defined by

$$\begin{aligned} \nabla u &= \nabla u \quad \forall u \in \Lambda_h^0 \\ \nabla v &= \text{rot}_h^* v \quad \forall v \in \Lambda_h^1 \\ \nabla(u\omega) &= 0 \quad \forall (u\omega) \in \Lambda_h^{2,*} . \end{aligned}$$

The co-differential operator δ is defined by $\delta := *d* : \Lambda_h^{2,*} \rightarrow \Lambda_h^{1,*} = \Lambda_h^1 \rightarrow \Lambda_h^0$, that is

$$\begin{aligned} \delta u &:= 0 \quad \forall u \in \Lambda_h^0 \\ \delta v &:= \text{div}_h v \quad \forall v \in \Lambda_h^1 \\ \delta(u\omega) &:= J\nabla u \quad \forall (u\omega) \in \Lambda_h^{2,*} . \end{aligned}$$

Both operators are similarly defined on $\Lambda_h^{0,*}$ respectively Λ_h^2 using rot_h respectively div_h^* .

We remind that in the smooth situation for a vector field $v = (v_1, v_2)$, we have $\nabla v = (v_{2|x} - v_{1|y})\nabla x \nabla y$ and $\delta v = v_{1|x} + v_{2|y}$ on a planar Euclidean domain with coordinates (x, y) .

Lemma 4. Let $u \in \Lambda^0$ and $w \in \Lambda^2$ then

$$\nabla^2 u(m) = 0 \text{ and } \delta^2 w(m) = 0 \text{ at each edge midpoint } m \in M_h .$$

Similarly, if $u \in \Lambda^{0,*}$ and $w \in \Lambda^{2,*}$ then

$$\nabla^2 u(p) = 0 \text{ and } \delta^2 w(p) = 0 \text{ at each interior vertex } p \in M_h ,$$

Proof. Direct consequence of the corollaries of the previous section.

We now state a Hodge-type decomposition of 1-forms (vector fields) on simplicial surfaces into a rotation-free, divergence-free, and a harmonic field.

Theorem 5. *Let M_h be a simplicial surface. Then any tangential vector field $\xi \in \Lambda^1(M_h)$ has a unique decomposition*

$$\xi = \nabla u + \delta(w\omega) + v \quad (8)$$

with $u \in \Lambda^0$, $w\omega \in \Lambda^2$ and harmonic component $v \in \Lambda^1$ with $\operatorname{div}_h v = \operatorname{rot}_h v = 0$, i.e. $\nabla v = 0$, $\delta v = 0$. Uniqueness of the decomposition follows from the normalization

$$\int_{M_h} u = 0, \quad \int_{M_h} w\omega = 0.$$

Since u and w are functions, ∇u is rotation-free and $\delta(w\omega)$ is divergence-free.

Proof. First, we derive the potential $u \in \Lambda^0$ of the rotation-free component of a given vector field ξ . We define the following quadratic functional F for functions in S_h

$$F(u) := \int_{M_h} (|\nabla u|^2 - 2 \langle \nabla u, \xi \rangle) \quad (9)$$

which associates a real-valued energy to each function u_h . A quadratic functional has a unique minimizer which we denote with $u \in S_h$. As a minimizer, u is a critical point of the functional which fulfills at each vertex p the following minimality condition

$$0 \stackrel{!}{=} \frac{d}{du_p} F(u) = 2 \int_{\operatorname{star} p} \langle \nabla u - \xi, \nabla \varphi_p \rangle \quad (10)$$

where $\varphi_p \in S_h$ is the Lagrange basis function corresponding to vertex p . Formally, u solves the Poisson equation $\operatorname{div}_h \nabla u = \operatorname{div}_h \xi$ respectively $\Delta_h u = \delta \xi$.

To obtain the divergence-free component we define a similar functional

$$G(w) := \int_{M_h} (|\delta(w\omega)|^2 - 2 \langle \delta(w\omega), \xi \rangle) \quad (11)$$

and compute the potential $w \in S_h$ as its unique minimizer which solves

$$0 \stackrel{!}{=} \frac{d}{dw_p} G(w) = 2 \int_{\operatorname{star} p} \langle \delta(w\omega) - \xi, J \nabla \varphi_p \rangle. \quad (12)$$

Formally, w solves $\operatorname{rot}_h \delta(w\omega) = \operatorname{rot}_h \xi$ resp. $\Delta_h w = \nabla \xi$.

The harmonic remainder is defined as $v := \xi - \nabla u - J \nabla w$. Using the above relations and the fact that for a 2-form $w\omega \in \Lambda_h^2$ we have $\operatorname{div}_h^* \delta(w\omega) = 0$ which implies $\operatorname{div}_h \delta(w\omega) = 0$, one easily verifies

$$\operatorname{div}_h v(p) = \operatorname{div}_h (\xi - \nabla u) - \operatorname{div}_h \delta(w\omega) = 0.$$

And using the fact that for a function $u \in \Lambda_h^1$ we have $\operatorname{rot}_h^* \nabla u = 0$ which implies $\operatorname{rot}_h \nabla u = 0$, we obtain

$$\operatorname{rot}_h v(p) = \operatorname{rot}_h (\xi - \delta(w\omega)) - \operatorname{rot}_h \nabla u = 0.$$

Theorem 5 was stated without proof as Theorem 2 in [17] where it was not made clear enough that the remaining component v is harmonic with respect to the *vertex based* operators div_h and rot_h .

6 Decomposition Algorithm and Detecting Vector Field Singularities

For arbitrary tangential piecewise-constant vector fields on a simplicial (planar or curved) surface M_h . Let M_h again be a simplicial planar or curved surface and $\xi \in A_h^1$ a vector field on M_h . If M_h is a curved surface, ξ is given by a constant vector in each triangle that lies in the triangle's plane. We now apply the discrete Hodge-Helmholtz decomposition introduced in the previous sections to split the given vector field into a rotation-free, a divergence-free, and a remaining harmonic component. The first component is the gradient field of a function u , and the second component is the co-gradient field, i.e. the gradient rotated with J by 90 degree, of a second function w . The decomposition is obtained by directly computing the functions as minimizers of the energy functionals above.

The steps for a practical decomposition of a vector field are now straightforward. Assume, we want to compute the rotation-free component of a given vector field ξ on a simplicial surface M_h with boundary. We begin with an arbitrary initial function $u_0 \in S_h$. The functional F in (10) is a quadratic in ∇u , so the minimization problem has a unique solution for ∇u (independent of the initial function u_0), and two solutions u differ only in a constant vertical offset. Since the offset has no effect on the critical points of u one can use any initial function u_0 . In practice we usually start with zero values everywhere. Then we apply a standard conjugate gradient method to minimize the energy functional F by modifying the function values of u_0 . As a result we obtain the a minimizer u of F . The same approach using the functional G is performed to compute the second potential w . Note that the minimization processes can be performed independently and simultaneously, e.g. on two different processors.

Furthermore, the minimization can be speed up rapidly by precomputing all terms which solely depend on the domain surface M_h , because only a few terms in the functionals and their gradients depend on the free variables. The evaluation of the gradient of the functional F in (10), for example, can be made rather efficient using the explicit representation of the discrete divergence operator given in (7):

$$\begin{aligned} \frac{d}{du_p} F(u) &= 2 \int_{\text{star } p} \langle \nabla u - \xi, \nabla \varphi_p \rangle \\ &= \sum_{i=1}^k (\cot \alpha_i + \cot \beta_i) \langle \nabla u - \xi, a_i \rangle . \end{aligned}$$

Since the cotangent values belong to the triangulation M_h their non-linear computation can be done in a pre-processing step once before the conjugate gradient method starts. Precomputing the scalar products of the vector field ξ with the edges a_i is also possible. During runtime of the conjugate gradient method it computes repeatedly per vertex the k scalar products $\langle \nabla u, a_i \rangle$ and k scalar multiplications and one addition, where k is the number of triangles in the star of the vertex p .

The vector field components of ξ are easily derived by differentiating the potentials. For efficiency, one does not need to store the three vector field components explicitly since they are explicitly determined by the scalar-valued potentials u and w . Further, if one is interested only, say, in identifying the vortices of a vector field ξ , then it suffices to calculate w and to avoid the calculation of the full decomposition. Note that if one only stores the two potentials and the remaining harmonic component v of the vector field, then one is still able to fully reconstruct the original vector field ξ using the decomposition equation (8).

The following algorithm describes how to identify singularities of a given vector field ξ :

Algorithm 6 (Identifying Singularities)

1. Calculate the potential u by minimizing the functional (9). The gradient of u is the rotation-free component of ξ .
2. Locate the local maxima and minima of the scalar valued function u over the two-dimensional surface, which are the centers of sinks or sources respectively. The maxima and minima can be automatically detected by searching for vertices p whose function value $u(p)$ is smaller or larger than the function values of all vertices on its link:

$$\begin{aligned} p \text{ is a sink} &\Leftrightarrow u(p) < u(q) \quad \forall q \in \partial \text{star } p \\ p \text{ is a source} &\Leftrightarrow u(p) > u(q) \quad \forall q \in \partial \text{star } p. \end{aligned}$$

A similar algorithm determines first-order vortices of the vector field ξ :

- 1'. Calculate the potential w by minimizing the functional (11).
- 2'. Locate the local maxima and minima of the potential w on the surface M_h which are the centers of vortices. Vortex rotation direction is determined by the type of extremal point (maximum or minimum).

$$p \text{ is a vortex} \Leftrightarrow u(p) < \text{ or } > u(q) \quad \forall q \in \partial \text{star } p.$$

Local methods for vortex identification and feature analysis of discrete vector fields often try to approximate the Jacobian by discrete differences or by higher-order interpolation of the vector field. This approach often suffers from numerical or measured inaccuracies of the vector field which make it a delicate task to extract higher order data such as the Jacobian or even higher order differential tensors.

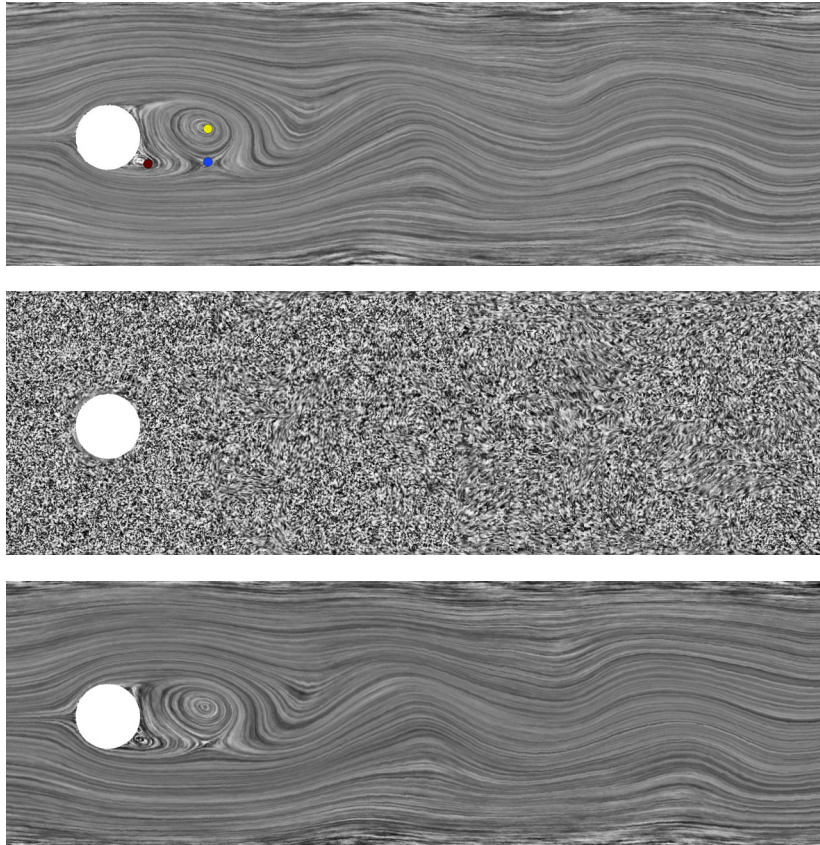


Fig. 4. Incompressible flow around a cylinder (bottom) with divergence-free (top), harmonic (middle) and vanishing rotation-free component. Two dots in the divergence-free part are the centers of rotation (white=clockwise, black=counter clockwise), and a third dot marks a saddle. All singularities were detected automatically by our method.

Our approach is global in the sense that u is rather independent of small local variations of the vector field which might have been introduced by numerical errors in the simulation, during the measurement, or by deficiency from a bad triangle mesh. This global approach is mainly due to the use of integrated values during the minimization of the functional.

7 Examples

The first example in Fig. 3 is an artificial vector field, by 90° degrees. The field is the sum of a gradient vector field and two co-gradient fields. Application of the Hodge decomposition leads to two potentials u and w with gradient ∇u

and co-gradient $J\nabla w$ shown in the upper two images on the left and right. The location of the original, generating potentials are indicated by dots. The algorithm detects the singularities and clearly separates the source from the two vortices. The centers of the potentials may be varied at interactive speed since on a smaller grid the decomposition is done in real-time as shown at the web site [14].

In Fig. 4 the decomposition is applied to an incompressible flow around a cylinder from a CFD simulation. The rotation-free component of the incompressible flow vanishes as expected. The harmonic component shows the incompressible, non-rotational part of the flow.

The flow in the Bay of Gdansk in Fig. 6, a coastal region in Poland, is data from a simulation performed at WL | Delft Hydraulics using a curvilinear grid of $43 * 28 * 20$ nodes. The goal of the simulation was to investigate the flow patterns induced by wind and several inflows. In [19] Sadarjoen and Post derive geometric quantities from curvature properties of streamlines to find vortex cores and analyze their qualitative behaviour. We computed the potentials of the gradient and co-gradient components and easily recovered the vortices. We also detected some sinks and sources, that come from vertical flows in the originally three-dimensional vector field.

The harmonic component of a vector field corresponds to an incompressible, irrotational flow. On compact surfaces this harmonic component represents the non-integrable flows around the handles of the surface. The artificial vector field in Fig. 1 is obtained from the restriction of the tangent field of a rotation of 3-space onto the pretzel. Around each handle we see a well-distinguished harmonic flow. There are also two sinks and two sources at the upper side and the lower side.

8 Conclusions and Future Work

We present a method for feature detection that is mathematically well founded and that adopts the discrete nature of experimental data. It succeeds in the detection of first order singularities. The two potentials we compute seem to hold much more information than we discussed in this paper. Therefore it is interesting to extract, for example, magnitudes, axes and angular velocities of vortices and strengths of sources/sinks from them. Since our variational approach is based on integrated values it has a smoothing effect on the potentials u and w , which is a good property for the detection of higher order critical points of these potentials. Work in these directions has been done and will be presented in a future paper.

Acknowledgments

The numerical flows were contributed by different sources. The simulation data of the Bay of Gdansk with courtesy WL|Delft Hydraulics and the help of

Frits Post and Ari Sadarjoen. The flow around a cylinder by Michael Hinze at Technische Universität Berlin. The numerical computations and visualizations are performed in JavaView [16] and are available at <http://www.javaview.de>.

References

1. D. Banks and B. Singer. A predictor-corrector technique for visualizing unsteady flow. *IEEE Transactions on Visualization and Computer Graphics*, 1(2):151–163, June 1995.
2. A. Bossavit. Mixed finite elements and the complex of whitney forms. In J. Whiteman, editor, *The Mathematics of Finite Elements and Applications VI*, pages 137–144. Academic Press, 1988.
3. A. Bossavit. *Computational Electromagnetism*. Academic Press, Boston, 1998.
4. S. C. Brenner and L. R. Scott. *The Mathematical Theory of Finite Element Methods*. Springer Verlag, 1994.
5. A. J. Chorin and J. E. Marsden. *A Mathematical Introduction to Fluid Mechanics*. Springer Verlag, 1998.
6. P. Ciarlet. *The Finite Element Method for Elliptic Problems*. North-Holland, 1978.
7. J. Dodziuk. Finite-difference approach to the hodge theory of harmonic forms. *Amer. J. of Math.*, 98(1):79–104, 1976.
8. B. Eckmann. Harmonische funktionen und randwertaufgaben in einem komplex. *Commentarii Math. Helvetici*, 17:240–245, 1944–45.
9. J. Helman and L. Hesselink. Representation and display of vector field topology in fluid flow data sets. *IEEE Computer*, 22(8):27–36, August 1989.
10. J. Helman and L. Hesselink. Visualizing vector field topology in fluid flows. *IEEE Computer Graphics & Applications*, 11(3):36–46, 1991.
11. H. Helmholtz. Über Integrale der Hydrodynamischen Gleichungen. *J. Reine Angew. Math.*, 55:25–55, 1858.
12. D. Kenwright and R. Haimes. Vortex identification - applications in aerodynamics: A case study. In R. Yagel and H. Hagen, editors, *Proc. Visualization '97*, pages 413 – 416, 1997.
13. U. Pinkall and K. Polthier. Computing discrete minimal surfaces and their conjugates. *Experim. Math.*, 2(1):15–36, 1993.
14. K. Polthier. JavaView homepage, 1998–2002. <http://www.javaview.de/>.
15. K. Polthier. Computational aspects of discrete minimal surfaces. In D. Hoffman, editor, *Proc. of the Clay Summerschool on Minimal Surfaces*. AMS, 2002.
16. K. Polthier, S. Khadem-Al-Charieh, E. Preuß, and U. Reitebuch. Publication of interactive visualizations with JavaView. In J. Borwein, M. H. Morales, K. Polthier, and J. F. Rodrigues, editors, *Multimedia Tools for Communicating Mathematics*, pages 241–264. Springer Verlag, 2002. <http://www.javaview.de>.
17. K. Polthier and E. Preuß. Variational approach to vector field decomposition. In R. van Liere, F. Post, and et.al., editors, *Proc. of Eurographics Workshop on Scientific Visualization*. Springer Verlag, 2000.
18. M. Roth and R. Peikert. A higher-order method for finding vortex core lines. In D. Ebert, H. Hagen, and H. Rushmeier, editors, *Proc. Visualization '98*, pages 143 – 150. IEEE Computer Society Press, 1998.

19. I. A. Sadarjoen and F. H. Post. Geometric methods for vortex extraction. In E. Gröller, H. Löffelmann, and W. Ribarsky, editors, *Data Visualization '99*, pages 53 – 62. Springer Verlag, 1999.
20. I. A. Sadarjoen, F. H. Post, B. Ma, D. Banks, and H. Pagendarm. Selective visualization of vortices in hydrodynamic flows. In D. Ebert, H. Hagen, and H. Rushmeier, editors, *Proc. Visualization '98*, pages 419 – 423. IEEE Computer Society Press, 1998.
21. G. Scheuermann, H. Hagen, and H. Krüger. Clifford algebra in vector field visualization. In H.-C. Hege and K. Polthier, editors, *Mathematical Visualization*, pages 343–351. Springer-Verlag, Heidelberg, 1998.
22. D. Sujudi and R. Haimes. Identification of swirling flow in 3-d vector fields. Technical report, Technical report, AIAA Paper 95-1715, 1995.
23. M. Tittgemeyer, G. Wollny, and F. Kruggel. Visualising deformation fields computed by non-linear image registration. *Computing and Visualization in Science*, 2002. to appear.
24. R. Westermann, C. Johnson, and T. Ertl. Topology preserving smoothing of vector fields. *Trans. on Vis. and Comp. Graphics*, pages 222–229, 2001.
25. H. Whitney. *Geometric Integration Theory*. Princeton University Press, 1957.
26. T. Wischgoll and G. Scheuermann. Detection and visualization of closed streamlines in planar flows. *Trans. on Vis. and Comp. Graphics*, 7(2):222–229, 2001.

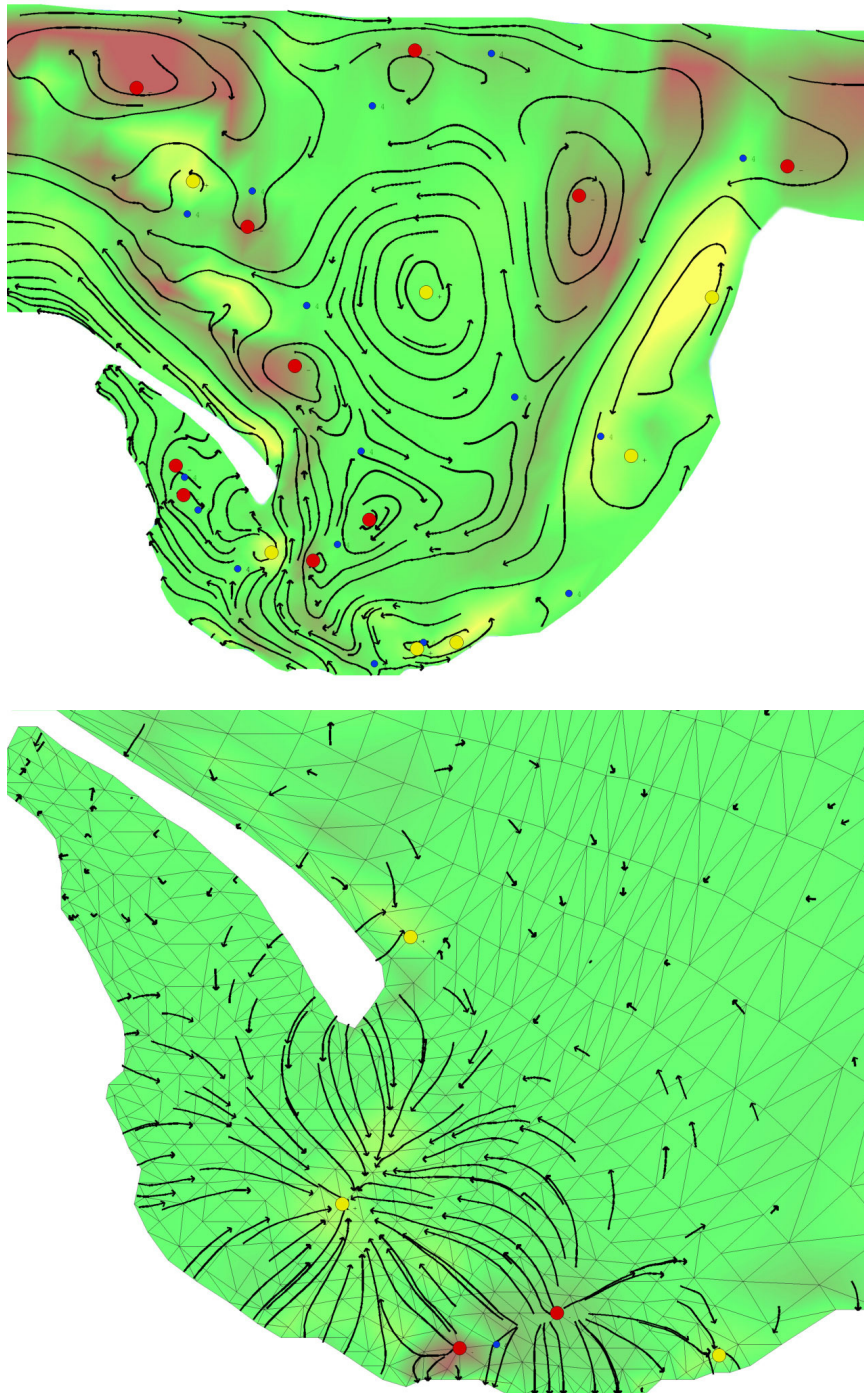


Fig. 5. Automatic identification of vector field singularities using a Hodge decomposition of a horizontal section of a flow in Bay of Gdansk. Rotation-free component (bottom) with sinks and sources, which come from vertical flows, and divergence-free component (top). The big dots indicate the location of sinks and sources (top) respectively vortices (bottom). The small dark dots mark saddle points (top and bottom). The bay is colorshaded by its discrete rotation (top) and divergence (bottom).

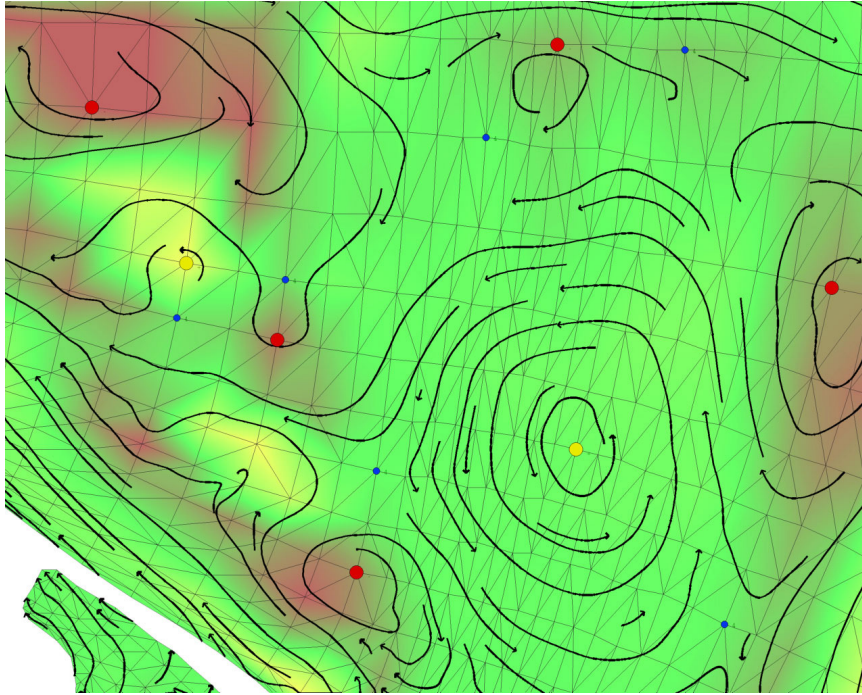


Fig. 6. Zoom into a region in Bay of Gdansk showing the divergence-free component of the Hodge decomposition with its integral curves. Big dots indicate locations of left and right rotating vortices, and small dark dots mark saddle points. The visualization of the vector field uses a vertex based, linear interpolated version of the element based vector field used for the decomposition, therefore sometimes there appear small discrepancies between visual centers of integral lines and indicated centers.